Using Protein Design To Dissect the Effect of Charged Residues on Metal Binding and Protein Stability†

Anna Wilkins Maniccia,‡ Wei Yang,‡ Shun-yi Li,‡ Julian A. Johnson,§ and Jenny J. Yang*,‡

Departments of Chemistry and Biology, Center for Drug Design and Biotechnology, Georgia State University, Atlanta, Georgia 30303

Received December 8, 2005; Revised Manuscript Received March 18, 2006

ABSTRACT: Ca^{2+} controls biological processes by interacting with proteins with different affinities, which are largely influenced by the electrostatic interaction from the local negatively charged ligand residues in the coordination sphere. We have developed a general strategy for rationally designing stable Ca^{2+}- and Ln^{3+}-binding proteins that retain the native folding of the host protein. Domain 1 of cluster differentiation 2 (CD2) is the host for the two designed proteins in this study. We investigate the effect of local charge on Ca^{2+}-binding affinity based on the folding properties and metal-binding affinities of the two proteins that have similarly located Ca^{2+}-binding sites with two shared ligand positions. While mutation and Ca^{2+} binding do not alter the native structure of the protein, Ca^{2+} binding specifically induced changes around the designed Ca^{2+}-binding site. The designed protein with a −5 charge at the binding sphere displays a 14-, 20-, and 12-fold increase in the binding affinity for Ca^{2+}, Tb^{3+}, and La^{3+}, respectively, compared to the designed protein with a −3 charge, which suggests that higher local charges are preferred for both Ca^{2+} and Ln^{3+} binding. The localized charged residues significantly decrease the thermal stability of the designed protein with a −5 charge, which has a T_m of 41 °C. Wild-type CD2 has a T_m of 61 °C, which is similar to the designed protein with a −3 charge. This decrease is partially restored by Ca^{2+} binding. The effect on the protein stability is modulated by the environment and the secondary structure locations of the charged mutations. Our study demonstrates the capability and power of protein design in unveiling key determinants to Ca^{2+}-binding affinity without the complexities of the global conformational changes, cooperativity, and multibinding process found in most natural Ca^{2+}-binding proteins.

Ca^{2+}-binding proteins are involved in numerous biological processes, both intra- and extracellularly (*1*, *2*). Ca^{2+} binding contributes to the folding and stability of proteins (e.g., in α-lactalbumin, thermitase, and thermolysin) (*3*). In the Ca^{2+}-dependent signal pathways, Ca^{2+} binding usually causes a large conformational change and leads proteins to interact with downstream partners or other target molecules. Because Ca^{2+} concentrations vary more than 10^4-fold in different cellular compartments and extracellular environments, Ca^{2+}-triggered proteins usually have Ca^{2+} affinities corresponding to the Ca^{2+} concentrations of their functional locations. In addition, a large number of Ca^{2+}-binding proteins play important roles in maintaining proper temporal and spatial distribution of the cellular Ca^{2+} concentration, preventing cells from Ca^{2+} overload and apoptosis (*4*). A number of transmembrane-spanning Ca^{2+}-binding proteins (e.g., cadherins and integrins) support the structural integrity of cells and tissues and contribute to the transduction of signals (*5*, *6*). Both stronger and weaker affinities hamper the protein functions by trapping them in either inactive or active states. Furthermore, mutations in Ca^{2+}-binding sites of proteins have been implicated in diseased states (*7*, *8*). Understanding the rules governing the Ca^{2+}-binding affinity not only facilitates studying Ca^{2+}-regulated biological processes and related diseases but also Ca^{2+}-mediated protein stability.

In proteins, Ca^{2+} predominantly uses oxygen atoms from the side chains of Asp, Glu, and Asn, the main chain, and solvent water as ligands (refers to the atom or residue chelating the Ca^{2+} throughout the paper). Several factors have been shown to be important in the binding of Ca^{2+}, such as the number of charged ligand residues, the binding geometry, and the protein environment (*9*−*13*). The number of acidic residues directly involved in binding has been proposed to be one of the most important factors contributing to Ca^{2+}-binding affinity and protein stability because of the electrostatic nature of Ca^{2+} binding. Sequence analysis of 165 EF-hand Ca^{2+} loops has shown that 6, 65, and 27% have net charges of −5, −4, and −3, respectively (*14*). Previous studies on the effect of primary coordination net charges on Ca^{2+} affinity have shown inconsistent results depending upon the protein used. Falke's group has shown that crowded negative ligands do not favor Ca^{2+} binding in the galactose-binding protein. Its original single Ca^{2+}-binding site with a net charge of −3 has a stronger binding affinity than the mutated site with a net charge of −4 (*15*, *16*). On the other hand, the same mutant significantly increased the metal-binding affinity for trivalent Tb^{3+} that has a similar ionic radius to Ca^{2+}. In contrast, Henzl et al. have shown that increasing the net negative charge in sites of α and β rat

† This work is supported in part by the MCB-0092486 (NSF) and GM 62999-1 and GM070555 (NIH) grants to J.J.Y. and NIH predoctoral fellowship to A.W.M.

* To whom correspondence should be addressed. Telephone: 404-651-4620. Fax: 404-651-2751. E-mail: chejjy@langate.gsu.edu.

‡ Department of Chemistry.

§ Department of Biology.

10.1021/bi052508q CCC: $33.50
Published on Web 04/15/2006

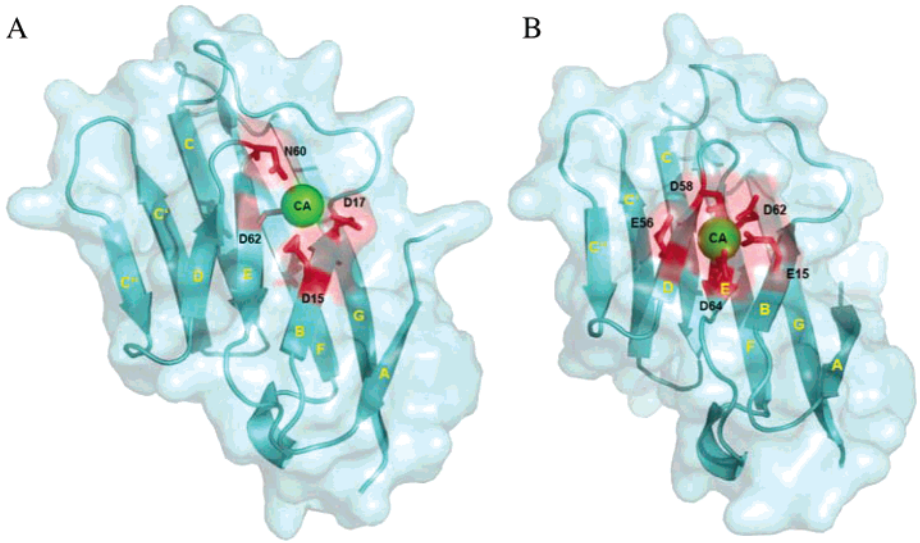

FIGURE 1: NMR structure of CD2.6D15 (A, 1T6W) and the model structure of CD2.7E15 (B). The Ca^{2+} is shown in green, and the ligand residues are in red. The residues are labeled in black, and the β strands are labeled in yellow. The pictures are generated using PyMol (DeLano Scientific LLC).

parvalbumins from −4 to −5 in the coordination sphere increases Ca^{2+} affinity (*17*). Such diversified results are likely due to the fact that the charged residues in these proteins contribute not only to the Ca^{2+} binding but also to the conformation and stability of the proteins in addition to the cooperative interaction of multiple Ca^{2+}-binding sites. Furthermore, using peptide models to dissect charge contribution to the Ca^{2+} affinity often suffers from the lack of well-defined conformations in solutions (*18*−*21*). Therefore, to date, the quantitative description of electrostatic effects in the primary coordinations to the Ca^{2+}-binding affinity remains to be established. A model system with minimized conformational change is advantageous in dissecting the contributions of different key factors that contribute to calcium-binding proteins.

Our lab has developed a design approach to create a single metal-binding site in a host protein, which surpasses the difficulties in multisite systems (*21*−*23*). We have shown that the majority of natural Ca^{2+}-binding sites in proteins share common pentagonal bipyramid geometry. In this study, two designed proteins termed CD2.6D15 and CD2.7E15 in the host protein domain 1 of cluster differentiation 2 (CD2)[1] were used to investigate the effect of local charges on the Ca^{2+}-binding affinity. We have reported that CD2.6D15 [termed Ca.CD2 in previous literature (*22*, *23*)] exhibits Ca^{2+} binding and metal selectivity. It also retains the native structure and cell-adhesion function of the host protein. The structural studies have shown that Ca^{2+} binds to the proposed location and binding ligands. Moreover, no significant conformational changes were induced by Ca^{2+} binding (Figure 1A), validating our design strategy (*22*, *23*).

In this study, we demonstrate the success of applying the established approach to create proteins with similar Ca^{2+}-binding environments differing in primary coordination charges and ligand types to dissect their contributions on the Ca^{2+}-binding affinity. We first report folding and metal-binding studies of two designed Ca^{2+}-binding proteins. While these two proteins have similar native structures, they exhibit more than 10-fold differences in metal-binding affinities. Although the native folding and conformation are not altered by the introduction of five negatively charged ligand residues at the Ca^{2+}-binding site, the thermal stability of the protein is significantly decreased in the absence of metal ions and partially restored by metal binding. Therefore, this system allows us to understand the role of local charge interactions to Ca^{2+} affinity and protein stability without the complexity of metal-induced conformational change observed in natural Ca^{2+}-binding proteins.

MATERIALS AND METHODS

Rational Design of Ca^{2+}-Binding Sites. A computer algorithm was used to design isolated Ca^{2+}-binding sites in a scaffold protein as previously described (*21*, *23*, *24*). Glu or Asp was used as the bidentate anchor, and three or four additional ligands were included for CD2.6D15 or CD2.7E15 design, respectively.

Protein Engineering. The cloning and purification of the proteins used classical methods described earlier (*21*, *23*). All solutions were treated with Chelex-100 resin (BioRad) to remove trace metal ions. Metal-free protein samples contain 1 mM ethylene glycol bis(2-aminoethyl ether)-*N*,*N*,*N*′,*N*′-tetraacetic acid (EGTA), except for the metal titrations.

Conformational Analysis. The conformation of the protein was investigated by circular dichroism (CD), fluorescence, and nuclear magnetic resonance (NMR) using the established methods (*21*, *23*). The samples for CD and Trp fluorescence are in 10 mM Tris at pH 7.4. The samples for Tb^{3+} fluorescence resonance energy transfer (FRET) and NMR are in 20 mM piperazine-1,4-bis(2-ethanesulfonic acid) (PIPES) and 10 mM KCl at pH 6.8 to avoid precipitation.

Thermal Stability. Thermal stability was measured by monitoring the CD signal change of the proteins in 10 mM Tris and 10 mM KCl at pH 7.5 from 5 to 95 °C. The signal changes (225 nm for CD2.7E15 and 230 nm for CD2.6D15) were fitted using the equation: $\Delta S = \Delta S_{max}/(1 + e^{(T_m - T)/k})$ to obtain the thermal transition point, where ΔS and ΔS_{max}

[1] Abbreviations: CD, circular dichroism; CD2, domain 1 of cluster differentiation 2; FRET, fluorescence resonance energy transfer.

are the signal changes at each data point and final point, T_m and T are the transition temperature and experimental temperature, respectively, and k is a transition rate that defines how fast the temperature-induced change occurs, which is represented by the slope of the transition phase in the fitting curve. A smaller k results in a sharper transition.

Metal Binding. The metal-binding properties were investigated by fluorescence and NMR as described earlier (*21*, *23*). The Tb^{3+}-binding affinity was measured using aromatic residue−Tb^{3+} FRET by monitoring the fluorescence increase at 545 nm versus the Tb^{3+} concentration. The La^{3+}-binding affinity was derived using the competitive binding of Tb^{3+} and La^{3+}. The protein concentrations for the Tb^{3+} titrations were ~2 and ~3 μM for 7E15 and 6D15, respectively, and the final Tb^{3+} concentrations were ~3 μM for CD2.7E15 and ~120 μM for CD2.6D15. For the La^{3+} competition study, La^{3+} was gradually added to the protein−Tb^{3+} mixture with ~2 and ~4 μM of 7E15 and 6D15, respectively, and ~2 μM (for CD2.7E15) and >20 μM (for CD2.6D15) of Tb^{3+}. The La^{3+} concentrations of the final points are >25 μM (for CD2.7E15) and >75 μM (for CD2.6D15). The data fit well using Specfit/32 (Spectrum Software Associates). Because of the significantly weaker affinity for Ca^{2+} than for Tb^{3+}, the Ca^{2+}-binding affinity cannot be obtained accurately using the Tb^{3+} FRET competitive binding assay. Therefore, the Ca^{2+}-binding affinity was measured using ^{15}N-^{1}H heteronuclear single-quantum coherence (HSQC) spectra by titrating Ca^{2+} into the protein samples (150 μM) with 40−50 μM EGTA at the initial point. The Ca^{2+} was gradually added, and the concentration of the final titration point is 13.1 mM. The dissociation constant was derived by monitoring the chemical-shift changes of several resonances versus the Ca^{2+} concentrations. Ca^{2+} binding resulted in the resonance changes around the designed Ca^{2+}-binding pocket in CD2.7E15, such as G61, D58, and Q22, in a fast phase with a K_d of 100 ± 50 μM. The K_d is the average of the results from several resonances, and the uncertainty represents the different responses of these resonances to the Ca^{2+} binding. A slower change with a K_d of more than 1 mM was observed for other residues such as E99 and L98 at the C terminus. This binding process is likely due to nonspecific binding because the residues that showed large chemical-shift changes at high Ca^{2+} concentrations are not geometrically clustered. On the other hand, residues of CD2.6D15 that exhibit chemical-shift changes are clustered around the Ca^{2+}-binding site, although they have a weak affinity with a K_d of 1.4 mM. Therefore, both CD2.7E15 and CD2.6D15 contain a single Ca^{2+}-binding site.

Electrostatic Potential Calculations. The electrostatic potentials were calculated using DelPhi (*25*−*27*). The calculation for CD2.7E15 and its variants is based on the model structures generated from the CD2 structure 1HNG. The calculation for CD2.6D15 is based on the solution structure 1T6W. The hydrogen atoms were built using SYBYL. The potentials in the presence and absence of Ca^{2+} are calculated by adding or removing the Ca^{2+} ions in the structure files without altering the coordinations of other atoms. The interior and exterior dielectric constants of 2 and 80, respectively, were used in DelPhi (*25*−*27*). The salt concentration was 0.01 M, and the linear solution of the Poisson−Boltzmann equation was imposed until convergence was reached.

RESULTS

Design of Ca^{2+}-Binding Proteins with Different Ligand Charge Numbers. We have analyzed 44 representative Ca^{2+}-binding proteins from different families out of the 515 Ca^{2+}-binding proteins in the Protein Data Bank (PDB). These detailed structural analyses have revealed that the average Ca^{2+}-binding ligand number is 6.5, and it often includes one to two ligands supplied by the solvent (*28*). Therefore, two novel Ca^{2+}-binding sites have been designed in CD2 with a total protein ligand number of either 6 or 5 as well as one or two possible solvent ligands. CD2.7E15 contains three mutations (N15E, L58D, and K64D) and two natural residues as ligands (E56 and D62). CD2.6D15 contains two mutations (N15D and N17D) and two natural residues as ligands (N60 and D62). E15 or D15 was proposed to serve as the bidentate ligand, respectively (Figure 1). CD2.7E15 and CD2.6D15 share two ligand positions (15 and 62) and a similar protein environment. The solvent accessibility of the ligand residues has only small differences revealed by GetArea (http://www.scsb.utmb.edu/cgi-bin/get_a_form.tcl) for the two proteins. The solvent accessibility of the bound Ca^{2+} is greater in CD2.6D15 than that in CD2.7E15 because the site in CD2.6D15 has one less ligand residue and uses D/N as ligands instead of E/Q with longer side chains. CD2.7E15 has a net charge of −5, while CD2.6D15 has a net charge of −3 in the metal-binding pockets. They are located on the BED surface of CD2, which is on the opposite face from the CD48-interaction GFCC′C″ face. The BED surface is less charged than the GFCC′C″ face (*29*) with only one and three charged residues on this surface not directly involved in the metal binding for CD2.7E15 (K66) and CD2.6D15 (E56, K64, and K66), respectively.

Two Designed Ca^{2+}-Binding Proteins Retain the Native Structure. The introduction of Ca^{2+} ligands in CD2 has not disturbed the protein structure as revealed by far-UV CD, fluorescence, and NMR. A single negative maximum at 216 nm was observed in CD spectra for both proteins (Figure 2A), indicating well-folded β-strand secondary structures. The fluorescence spectra showed an emission maximum at 327 nm (Figure 2B), which arises from the buried Trp-32 in the hydrophobic environment. In addition, 1D ^{1}H NMR spectra of CD2.7E15 and CD2.6D15 are very similar to that of CD2 with widely dispersed resonances. These results indicated that CD2.7E15 has similar secondary structure and tertiary packing to that of CD2.6D15 and CD2 (*22*, *23*). The addition of Ca^{2+} and Ln^{3+} ions induced negligible differences in the CD and fluorescence spectra as well as the overall NMR spectra. However, several resonances around the metal-binding pockets such as Gly-61 underwent relatively large shifts upon the addition of Ca^{2+} (Figure 3), suggesting that only local conformational changes occur upon metal binding.

Metal-Binding Affinities. The metal-binding properties of CD2.6D15 and CD2.7E15 have been investigated using aromatic residue−Tb^{3+} FRET and NMR (Figure 3). Tb^{3+} shares coordination properties similar to Ca^{2+} and is often used to probe the Ca^{2+}-binding proteins (*30*, *31*). With the addition of CD2.6D15 or CD2.7E15 into Tb^{3+} solutions, the fluorescent signal at 545 nm dramatically increased (>20-fold), while the addition of CD2 resulted in an insignificant change, suggesting that the enhancement of Tb^{3+} signal originates from the binding to the designed proteins. Figure

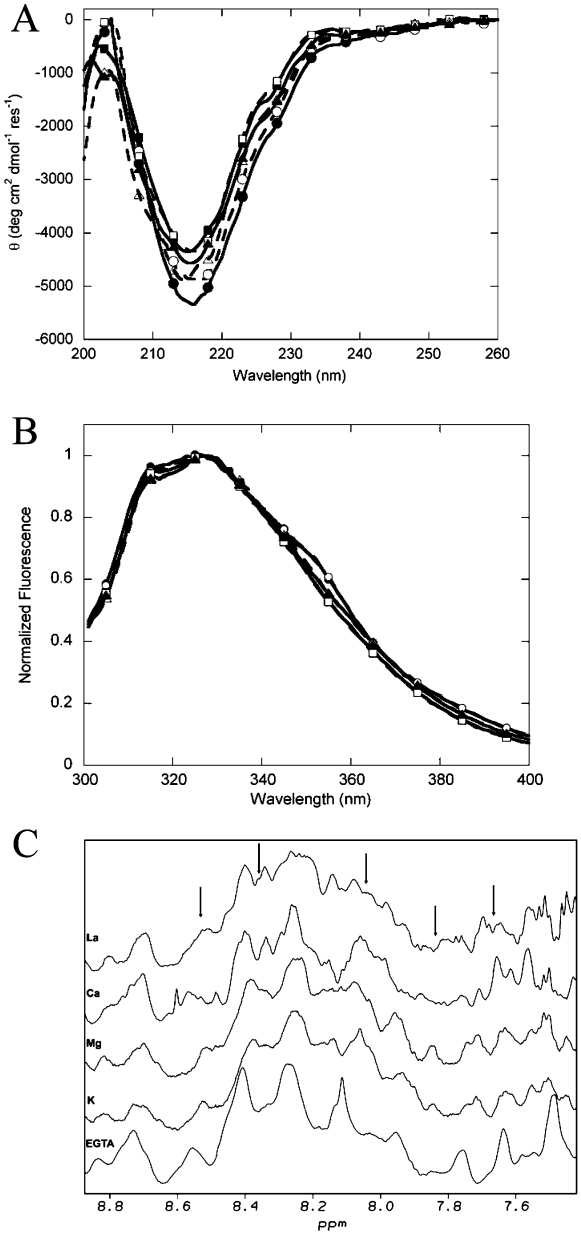

FIGURE 2: Far-UV CD (A) and Trp fluorescence spectra (B) of CD2.7E15 (▲ and △), CD2.6D15 (● and ○), and CD2 (■ and □) in the presence of 10 mM Ca^{2+} (▲, ■, and ●) or 1 mM EGTA (△, □, and ○). (C) One-dimensional NMR of CD2.7E15 with the sequential addition of different metal ions (from bottom to top). The final concentrations are 0.05 mM for EGTA, 130 mM for K^+, 10 mM for Mg^{2+}, 5 mM for Ca^{2+}, and 1 mM for La^{3+}. The arrows indicate the Ca^{2+}-induced change.

3B shows that La^{3+} competes with the Tb^{3+} binding to reduce the fluorescence intensity. In contrast, excess concentrations of K^+ (130 mM) and Mg^{2+} (10 mM) have only minor effects. Similarly, Ca^{2+} and La^{3+} in the presence of high concentrations of Mg^{2+} and K^+ are able to induce specific resonance changes in the NMR spectra (Figure 2C). The results suggest that CD2.6D15 and CD2.7E15 selectively bind to the Ca^{2+} and Ln^{3+} over the excess physiological cations Mg^{2+} and K^+.

The metal-binding affinities for Tb^{3+} and La^{3+} are 8 ± 2 and 6 ± 3 μM for CD2.6D15 and 0.4 ± 0.2 and 0.5 ± 0.1 μM for CD2.7E15, respectively, using direct Tb^{3+} titration into the protein and the La^{3+} titration into the Tb^{3+}−protein complex, respectively. The Ca^{2+}-binding affinity of CD2.6D15 is 1400 ± 400 μM, derived from the chemical-shift changes of the residues proximate to the metal-binding position (*23*). Figure 3C shows the ^{1}H-^{15}N HSQC spectra of CD2.7E15 at different Ca^{2+} concentrations. Ca^{2+} binding specifically results in changes of the chemical shifts of the resonances around the designed Ca^{2+}-binding pocket such as G61 and D58 as well as Q22. A dissociation constant of 100 ± 50 μM was obtained using the residues around the designed Ca^{2+}-binding pocket. The dissociation constants for K^+ or Mg^{2+} are estimated to be greater than 10 mM for both proteins.

Thermal Stability. The effects of clustered charges on protein folding and stability have been investigated using far-UV CD. The spectra of both proteins at 25 or 85 °C overlap with that of CD2 (*32*), suggesting that they have similar native and thermally unfolded states. As shown in Figure 4, the changes of the CD signal versus the temperature consist of a two-state transition model. The melting point (T_m) of CD2.6D15 is ∼63 °C both in the presence of 1 mM EGTA or 10 mM Ca^{2+}, which is similar to that of CD2 (61 ± 1 °C) (*32*). The T_m of CD2.7E15 is 41 °C in the presence of 1 mM EGTA and 51 °C in the presence of 10 mM Ca^{2+}.

DISCUSSION

Using Designed Proteins To Dissect the Contribution of the Charge Effect for Ca^{2+} Binding and Stability. Extensive studies have been carried out to determine the contribution of different factors to Ca^{2+}-binding properties and protein stability (*9*, *10*, *12*, *13*, *33*−*35*). However, the contributions are difficult to dissect in natural proteins because of conformational change and multiple binding processes. For example, cooperative binding of two or four Ca^{2+} ions in calmodulin results in a global secondary-structure reorientation (*36*, *37*). The residues that are located either at the Ca^{2+} ligand, in the EF loop, or at distal locations all have differential effects on Ca^{2+} binding and conformational entropy in addition to the cooperative interaction of coupled metal-binding sites (*38*−*40*). The modification of the residues at one domain alters the metal-binding properties in the other domain and vice versa (*10*, *11*, *41*, *42*). Although Ca^{2+} buffer proteins, such as parvalbumin and calbindin$_{D9K}$, do not exhibit large Ca^{2+}-induced conformational changes, elegant studies carried out previously have shown that there is strong communication between coupled EF-hand motifs. The S55D mutation of parvalbumin not only increases the Ca^{2+}-binding affinity of the N-terminal Ca^{2+}-binding motif that it belongs to but also increases the affinity of the C-terminal motif (*17*). In calbindin$_{D9k}$, NMR studies have shown that the initial Ca^{2+} binding at either site induces the local conformations of both Ca^{2+}-binding motifs to be the Ca^{2+}-bound forms, although no global conformational change occurs (*43*). Peptide fragments encompassing Ca^{2+}-binding motifs and single Ca^{2+}-binding proteins, such as α-lactalbumin, are usually unfolded or partially unfolded in a molten-globule state in the absence of Ca^{2+} (*44*, *45*). Understanding key determinants for weaker Ca^{2+}-binding proteins such as C2 domain and cadherin with K_ds between 0.05 and 1.5 mM is even more challenging because several Ca^{2+}-binding sites are clustered together with shared ligand residues and high cooperativity (*46*−*49*).

We have shown that the Ca^{2+} binding to two designed proteins CD2.6D15 and CD2.7E15 does not change the

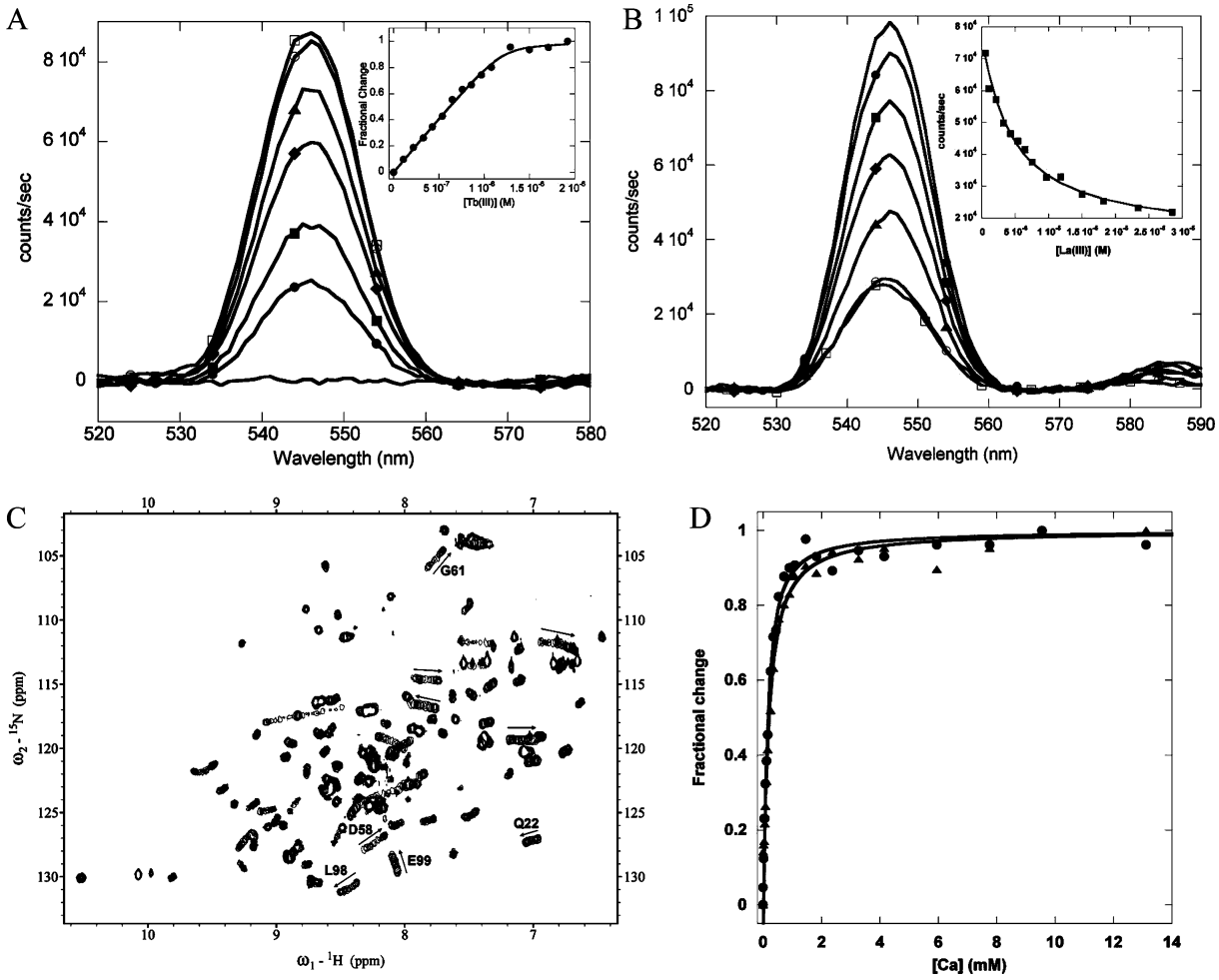

FIGURE 3: (A) Fluorescence intensity at 545 nm increases with the addition of Tb^{3+} into CD2.7E15 that gives the K_d of Tb^{3+} (inset). (B) Signal decreases with the addition of La^{3+} into the CD2.7E15−Tb^{3+} mixture that derives the K_d of La^{3+} (inset). (C) HSQC of CD2.7E15 at different Ca^{2+} concentrations. The arrows indicate the shift directions with the Ca^{2+}, and several residues are labeled. (D) Ca^{2+} affinity has been obtained by monitoring the chemical-shift changes versus the Ca^{2+} concentrations. The changes of two resonances corresponding to G61 (●) and Q22 (▲) are shown, and the binding affinity is the average of results from multiple resonances.

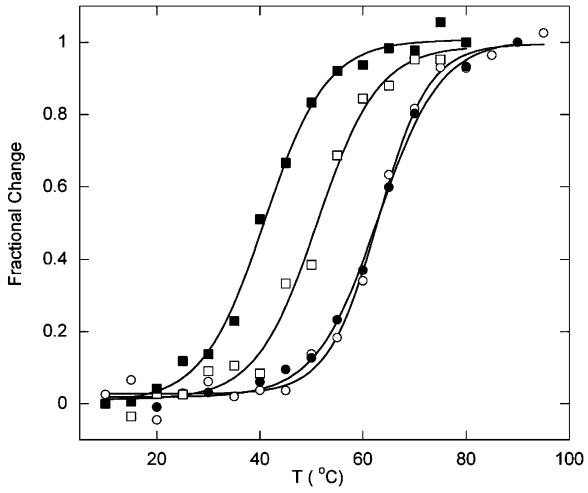

FIGURE 4: Thermal denaturation of CD2.6D15 (● and ○) and CD2.7E15 (■ and □) monitored at 230 and 225 nm by far-UV CD, respectively, as a function of the temperature in the presence of 10 mM Ca^{2+} (○ and □) and 1 mM EGTA (● and ■).

structure of the host protein, thus overcoming the limitation of natural Ca^{2+}-binding proteins. The NMR structures of CD2.6D15 have a root-mean-square deviation (rmsd) < 1.1 Å to that of CD2 (1HNG) (*23*). The structure of CD2.7E15 is similar as revealed by several spectroscopic methods (Figures 2 and 3). Furthermore, the addition of excess Ca^{2+} or Ln^{3+} did not induce global conformational changes. Our NMR studies of CD2.6D15 have shown that the small conformational and dynamic changes are localized around the Ca^{2+}-binding residues mainly at the loop regions, while residues not involved in metal binding at the β strands have negligible changes (*23*). Assuming the backbone entropy change induced by Ca^{2+} binding is small, which is indicated by the dynamic study of CD2.6D15 (*22*, *23*), the contribution of the binding energy is mainly provided by the metal−ligand interactions. Therefore, the effects of local factors such as charge ligand residues on the Ca^{2+} binding can be directly revealed without the complication of the naturally occurring Ca^{2+}-binding proteins.

Comparison of Affinities for CD2.6D15 versus CD2.7E15 to Different Metals. Although CD2.7E15 and CD2.6D15 exhibit similar structures and share two Ca^{2+} ligand positions, they possess 10−20-fold differences in metal-binding affinities. This difference arises mainly from the different charges, ligand types, ligand numbers, and binding coordination geometries. Although two proteins were designed using the same ideal binding geometry, the actual geometries in the engineered proteins may vary. In addition, CD2.6D15

Table 1: Metal-Binding Affinity and Thermal Stability of the Designed Proteins

protein	charges at binding site	K_d (μM)			T_m (°C)	
		Ca^{2+}	Tb^{3+}	La^{3+}	EGTA	Ca^{2+}
CD2					61 ± 1	61 ± 1
CD2.6D15	−3	1400 ± 400	8 ± 2	6 ± 3	63 ± 2	63 ± 2
CD2.7E15	−5	100 ± 50	0.4 ± 0.2	0.5 ± 0.1	41 ± 2	51 ± 2

utilizes four ligands from Asp or Asn, while CD2.7E15 utilizes five ligands including two Glu residues. The additional methylene group in Glu may provide more freedom for the Ca^{2+}-binding geometry. Without systematic studies, the effects from these factors cannot be excluded. Nevertheless, our finding that higher charged sites retain stronger Ca^{2+} and Tb^{3+} binding is similar to the finding in parvalbumin that the introduction of a fifth negative ligand at either EF-hand motif increased its Ca^{2+} affinity more than 10-fold (*17*). It is important to carry out a systematic dissection of charge effects on Ca^{2+}-binding affinity using designed proteins as the templates.

We have also shown that Tb^{3+} and La^{3+} have binding affinities about 100−200-fold stronger than that of Ca^{2+} in both proteins, which correlates to a binding energy difference of 3−5 kcal/mol. Ln^{3+} binding to metal-binding sites receives enhanced interests because of the use of Ln^{3+} ions in spectroscopic and crystallographic studies of biomolecules. It is particularly useful for Ca^{2+}-binding proteins because of the spectroscopic silence of Ca^{2+} and the similarity of the binding properties between Ca^{2+} and Ln^{3+} ions. In CD2.6D15 and CD2.7E15, the Ca^{2+}-binding sites are located at the protein surface and the ligands are not tightly restricted by their surroundings, which provide the required freedom for the geometric coordinations of the metal ions with different radii. Assuming the metal−ligand distance is optimized for the metal binding, Dudev et al. have shown, using small molecule models, that higher negative charge numbers favor the La^{3+} substitution of Ca^{2+} binding in a less exposed environment (*50*). Ca^{2+}-binding sites on the protein surface usually have a dielectric constant of 10−20 because of partial shielding by the carbon atoms next to the ligand oxygen atoms. Predicted energy differences because of La^{3+} substitution of Ca^{2+} with a −3 charge are 2.2 and 13.4 kcal/mol for dielectric constants of 10 and 20, respectively (*50*), which are consistent with the results reported here.

A similar increase in Tb^{3+} binding observed for the designed proteins by increasing the net charge at the metal-binding pocket has also been observed in the galactose-binding protein. The replacement of Q142 (position 9 of the EF-hand motif) with E or D increased the trivalent binding affinity 6- or 13-fold, respectively; however, the Ca^{2+} affinity of the galactose-binding protein is decreased more than 300- and 17-fold, respectively. Such a significant difference is likely due to the fact that the metal-binding site in the galactose-binding protein is largely restricted by the protein context based on the observation that its selectivity is dependent upon the ionic radii (*51*−*53*).

Implication of Charged Ligand Residues on Protein Stability. The clustering of five negatively charged residues in CD2.7E15 significantly decreases the thermal transition T_m value, while that of CD2.6D15 is not significantly affected by the clustering of three negatively charged residues (Table 1). The decreased thermal transition T_m value of CD2.7E15 is possibly a result from the destabilization of the native state and/or the stabilization of the unfolded state of the protein. The destabilization of the native state because of the electrostatic repulsion among charged ligand residues is supported by the calculation of the protein energy change based on the Poisson−Boltzmann relationship using DelPhi (*25*, *27*) (Figure 5). The three negative mutations result in a large free-energy change for CD2.7E15 (+296 kcal/mol), while the change of the calculated free energy of CD2.6D15 compared to CD2 is very small (+24 kcal/mol in the absence of Ca^{2+}). The calculated free-energy change for the residues 14−18 and 55−65 (including all of the ligands in CD2.6D15 and CD2.7E15 and their neighbors) is almost the same as that of the intact protein. Although the calculation can only be considered as semiquantitative, a free-energy enhancement of 296 kcal/mol strongly implies that the decrease of the protein stability in CD2.7E15 is due to introduced charge repulsion. We have further examined the effect of single mutations by restoring the three native residues individually in the model structure of CD2.7E15. The calculation results show that each mutation contributes significantly to the electrostatic repulsion and the clustering of negative charges

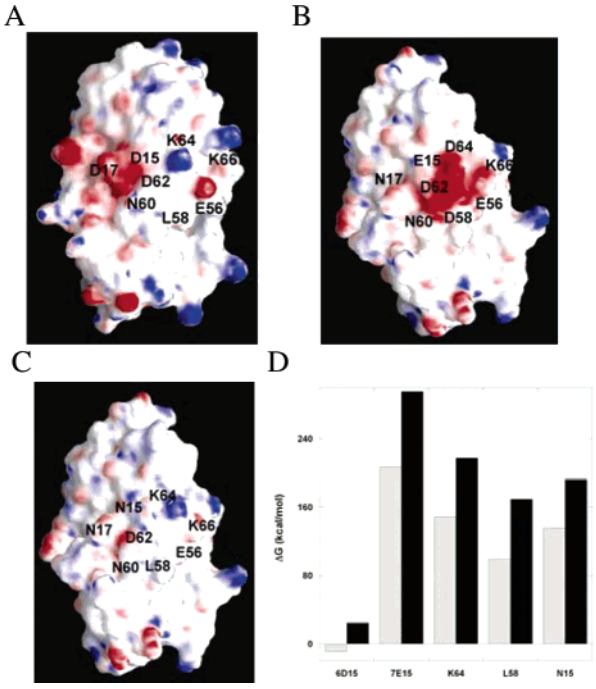

FIGURE 5: Surface potential of CD2.6D15 (A), CD2.7E15 (B), and CD2 (C) calculated by DelPhi. Negative potentials are red, and positive potentials are blue. (D) Free-energy change of CD2.6D15, CD2.7E15, and CD2.7E15 variants compared to CD2 provided by the DelPhi calculation. The K64, L58, and N15 are CD2.7E15 variants restoring the corresponding native residues while maintaining the other mutations in the model structures. The gray bars represent the Ca^{2+}-loaded form, and the black bars represent the Ca^{2+}-free form.

at the designed Ca^{2+}-binding site has a cumulative destabilization effect.

The degree of protein destabilization because of the introduction of charged ligand residues depends upon the protein environment. For example, the extent of interference in native electrostatic interactions, the flexibility of the residues introduced, and the secondary structure of the charge location may generate diverse effects on protein stability (*54*). The removal of the native attraction of K64−D62 and K64−E56 by the mutation K64D, to form the Ca^{2+}-binding site of CD2.7E15, also likely contributes to the larger free-energy change. In contrast, the creation of the Ca^{2+}-binding site of CD2.6D15 does not significantly alter the surrounding native charge−charge interactions. In addition, the bound Ca^{2+} in CD2.6D15 has a greater solvent accessibility than that in CD2.7E15 because the site in CD2.6D15 has one less ligand residue and uses D/N as ligands instead of E/Q with longer side chains. Further, two of the three negatively charged ligand residues in CD2.6D15 are in the flexible loop region, which enables the charged residues to adjust the local conformations that decrease the repulsion among them in the absence of Ca^{2+}. These cumulative effects are likely the reasons for an insignificant change in T_m of CD2.6D15 upon Ca^{2+} binding. In contrast, two charged mutations, T79D and A92E, at β-strand locations largely destabilize the thermal stability of CD2.6D79, a designed Ca^{2+}-binding protein with two negative residues at the binding pocket. Its T_m decreases to 47 °C in the absence of Ca^{2+} (Jones et al., unpublished data). The rigid backbone of the β sheet limits the conformation adjustment for lessening the charge repulsion. It is noteworthy that four charged residues (E15, D58, D64, and E56) of CD2.7E15 are located at the β strands with limited flexibility, which has an even stronger destabilization effect that results in a T_m of 41 °C. The metal partially neutralized the negative potentials in the binding pocket of CD2.7E15, which significantly restored its thermal stability by 10 °C. Ca^{2+} binding did not completely regain protein stability because the charge repulsion was only partially neutralized. These results indicate that the environment and the secondary-structure locations modulate the effect of clustered charges on protein stability.

A recent study by Schmid and colleagues has also revealed that the local charge variants and the context of the mutations are more important to the cold-shock protein stability than the net charges that were proposed in an earlier study (*55*−*57*). Henzl and Graham have also reported that the β-parvalbumin, with a net charge of −16, indeed displays a 7 °C higher T_m than the α-parvalbumin with a net charge of −5 (*58*, *59*). The study by Xiao and Honig has indicated that the electrostatic interactions function differently in different protein families (*60*). In the glutamate dehydrogenase family, Coulombic interactions of positive−negative ion pairs stabilize the protein. In the D-glyceraldehyde-3-phosphate dehydrogenase family, the charge−polar interaction contributes more to the stability. On the other hand, in the CheY and ferredoxin families, the determinant of the stability is from the desolvation free energy.

CONCLUSIONS

In summary, we have successfully designed two Ca^{2+}-binding proteins with different charge arrangement and similar binding location. The proteins specifically bind to Ca^{2+} and its analogues Tb^{3+} and La^{3+}. Because both proteins retain native structures and do not exhibit Ca^{2+}-induced conformational change, the contribution of local arrangement on the metal-binding affinity and protein stability can be directly revealed in a controlled manner without the complication of global conformational changes and cooperativity observed in natural Ca^{2+}-binding proteins. We have shown that CD2.7E15 with five negatively charged ligands has a 10−20-fold greater affinity for both Ca^{2+} and Ln^{3+}, respectively, than CD2.6D15 with three negatively charged ligands. Both proteins exhibit 100−200-fold greater affinity for Tb^{3+} and La^{3+} than that of Ca^{2+}. The introduction of negatively charged residues in CD2.7E15 significantly decreases the thermal stability. The effect of clustered charge residues on the protein stability is modulated by the environment and the secondary-structure locations. Both CD2.6D15 and CD2.7E15 are excellent model proteins for further systematic investigation of key factors involved in the determination of Ca^{2+}-binding affinity and protein stability that are currently underway. The principles obtained from such studies will provide insights not only into the diseases related to the malfunction of Ca^{2+} binding but also toward understanding Ca^{2+} signaling and designing Ca^{2+}-dependent functional proteins and thermally stable biomaterials. Furthermore, the preference for binding of Ln^{3+} and other paramagnetic metal ions by designed proteins has implications for structural determination of large protein complexes using docking protocols based on residual dipolar couplings.

ACKNOWLEDGMENT

The authors thank Dan Adams, Yiming Ye, Jin Zou, April Ellis, Lisa Jones, and other members in the research group of Dr. Jenny J. Yang for critical review and helpful discussion. The authors also thank Michael Kirberger and Homme Hellinga for PROTEUS and Dezymer.

REFERENCES

1. Strynadka, N. C., and James, M. N. G. (1993) Calcium-binding proteins, in *Encyclopedia of Inorganic Chemistry*, 1st ed. (King, R. B., Ed.) pp 477−507, John Wiley and Sons, Ltd., New York.
2. McPhalen, C. A., Strynadka, N. C., and James, M. N. (1991) Calcium-binding sites in proteins: A structural perspective, *Adv. Protein Chem. 42*, 77−144.
3. Glusker, J. P. (1991) Structural aspects of metal liganding to functional groups in proteins, *Adv. Protein Chem. 42*, 1−76.
4. Dowd, D. R. (1995) Calcium regulation of apoptosis, *Adv. Second Messenger Phosphoprotein Res. 30*, 255−280.
5. Downing, A. K., Knott, V., Werner, J. M., Cardy, C. M., Campbell, I. D., and Handford, P. A. (1996) Solution structure of a pair of calcium-binding epidermal growth factor-like domains: Implications for the Marfan syndrome and other genetic disorders, *Cell 85*, 597−605.
6. Maurer, P., Hohenester, E., and Engel, J. (1996) Extracellular calcium-binding proteins, *Curr. Opin. Cell Biol. 8*, 609−617.
7. McGettrick, A. J., Knott, V., Willis, A., and Handford, P. A. (2000) Molecular effects of calcium binding mutations in Marfan syndrome depend on domain context, *Hum. Mol. Genet. 9*, 1987−1994.
8. Rhyner, J. A., Durussel, I., Cox, J. A., Ilg, E. C., Schafer, B. W., and Heizmann, C. W. (1996) Human recombinant α-parvalbumin and nine mutants with individually inactivated calcium- and magnesium-binding sites: Biochemical and immunological properties, *Biochim. Biophys. Acta 1313*, 179−186.
9. Linse, S., Brodin, P., Johansson, C., Thulin, E., Grundstrom, T., and Forsen, S. (1988) The role of protein surface charges in ion binding, *Nature 335*, 651−652.

10. Linse, S., and Forsen, S. (1995) Determinants that govern high-affinity calcium binding, *Adv. Second Messenger Phosphoprotein Res. 30*, 89−151.
11. Linse, S., Helmersson, A., and Forsen, S. (1991) Calcium binding to calmodulin and its globular domains, *J. Biol. Chem. 266*, 8050−8054.
12. Wu, X., and Reid, R. E. (1997) Structure/calcium affinity relationships of site III of calmodulin: Testing the acid pair hypothesis using calmodulin mutants, *Biochemistry 36*, 8649−8656.
13. Wu, X., and Reid, R. E. (1997) Conservative D133E mutation of calmodulin site IV drastically alters calcium binding and phosphodiesterase regulation, *Biochemistry 36*, 3608−3616.
14. Marsden, B. J., Shaw, G. S., and Sykes, B. D. (1990) Calcium binding proteins. Elucidating the contributions to calcium affinity from an analysis of species variants and peptide fragments, *Biochem. Cell Biol. 68*, 587−601.
15. Falke, J. J., Drake, S. K., Hazard, A. L., and Peersen, O. B. (1994) Molecular tuning of ion binding to calcium signaling proteins, *Q. Rev. Biophys. 27*, 219−290.
16. Falke, J. J., Snyder, E. E., Thatcher, K. C., and Voertler, C. S. (1991) Quantitating and engineering the ion specificity of an EF-hand-like Ca^{2+} binding, *Biochemistry 30*, 8690−8697.
17. Henzl, M. T., Hapak, R. C., and Goodpasture, E. A. (1996) Introduction of a fifth carboxylate ligand heightens the affinity of the oncomodulin CD and EF sites for Ca^{2+}, *Biochemistry 35*, 5856−5869.
18. Demarest, S. J., Zhou, S. Q., Robblee, J., Fairman, R., Chu, B., and Raleigh, D. P. (2001) A comparative study of peptide models of the α-domain of α-lactalbumin, lysozyme, and α-lactalbumin/lysozyme chimeras allows the elucidation of critical factors that contribute to the ability to form stable partially folded states, *Biochemistry 40*, 2138−2147.
19. Demarest, S. J., Fairman, R., and Raleigh, D. P. (1998) Peptide models of local and long-range interactions in the molten globule state of human α-lactalbumin, *J. Mol. Biol. 283*, 279−291.
20. Reid, R. E. (1990) Synthetic fragments of calmodulin calcium-binding site III. A test of the acid pair hypothesis, *J. Biol. Chem. 265*, 5971−5976.
21. Yang, W., Jones, L. M., Isley, L., Ye, Y., Lee, H. W., Wilkins, A., Liu, Z. R., Hellinga, H. W., Malchow, R., Ghazi, M., and Yang, J. J. (2003) Rational design of a calcium-binding protein, *J. Am. Chem. Soc. 125*, 6165−6171.
22. Yang, W., Wilkins, A. L., Li, S., Ye, Y., and Yang, J. J. (2005) The effects of Ca^{2+} binding on the dynamic properties of a designed Ca^{2+}-binding protein, *Biochemistry 44*, 8267−8273.
23. Yang, W., Wilkins, A. L., Ye, Y., Liu, Z. R., Li, S. Y., Urbauer, J. L., Hellinga, H. W., Kearney, A., van der Merwe, P. A., and Yang, J. J. (2005) Design of a calcium-binding protein with desired structure in a cell adhesion molecule, *J. Am. Chem. Soc. 127*, 2085−2093.
24. Yang, W., Lee, H. W., Hellinga, H., and Yang, J. J. (2002) Structural analysis, identification, and design of calcium-binding sites in proteins, *Proteins 47*, 344−356.
25. Gilson, M. K., and Honig, B. (1988) Calculation of the total electrostatic energy of a macromolecular system: Solvation energies, binding energies, and conformational analysis, *Proteins 4*, 7−18.
26. Gilson, M. K., Rashin, A., Fine, R., and Honig, B. (1985) On the calculation of electrostatic interactions in proteins, *J. Mol. Biol. 184*, 503−516.
27. Honig, B., and Nicholls, A. (1995) Classical electrostatics in biology and chemistry, *Science 268*, 1144−1149.
28. Pidcock, E., and Moore, G. R. (2001) Structural characteristics of protein binding sites for calcium and lanthanide ions, *J. Biol. Inorg. Chem. 6*, 479−489.
29. Davis, S. J., Ikemizu, S., Wild, M. K., and van der Merwe, P. A. (1998) CD2 and the nature of protein interactions mediating cell−cell recognition, *Immunol. Rev. 163*, 217−236.
30. Horricks, W. D. (1993) in *Methods in Enzymology* (Riordan, J. F., and Vallee, B. L., Eds.) pp 495−538, Academic Press, Inc., New York.
31. Horrocks, W. D., Jr. (1982) Lanthanide ion probes of biomolecular structure, *Adv. Inorg. Biochem. 4*, 201−261.
32. Yang, J. J., Yang, H., Ye, Y., Hopkins, H., Jr., and Hastings, G. (2002) Temperature-induced formation of a non-native intermediate state of the all β-sheet protein CD2, *Cell Biochem. Biophys. 36*, 1−18.
33. Linse, S., Johansson, C., Brodin, P., Grundstrom, T., Drakenberg, T., and Forsen, S. (1991) Electrostatic contributions to the binding of Ca^{2+} in calbindin D9k, *Biochemistry 30*, 154−162.
34. Christodoulou, J., Malmendal, A., Harper, J. F., and Chazin, W. J. (2004) Evidence for differing roles for each lobe of the calmodulin-like domain in a calcium-dependent protein kinase, *J. Biol. Chem. 279*, 29092−29100.
35. Faga, L. A., Sorensen, B. R., VanScyoc, W. S., and Shea, M. A. (2003) Basic interdomain boundary residues in calmodulin decrease calcium affinity of sites I and II by stabilizing helix−helix interactions, *Proteins 50*, 381−391.
36. Finn, B. E., Evenas, J., Drakenberg, T., Waltho, J. P., Thulin, E., and Forsen, S. (1995) Calcium-induced structural changes and domain autonomy in calmodulin, *Nat. Struct. Biol. 2*, 777−783.
37. Maune, J. F., Beckingham, K., Martin, S. R., and Bayley, P. M. (1992) Circular dichroism studies on calcium binding to two series of Ca^{2+} binding site mutants of *Drosophila melanogaster* calmodulin, *Biochemistry 31*, 7779−7786.
38. Maler, L., Blankenship, J., Rance, M., and Chazin, W. J. (2000) Site−site communication in the EF-hand Ca^{2+}-binding protein calbindin D9k, *Nat. Struct. Biol. 7*, 245−250.
39. Spyracopoulos, L., Gagne, S. M., Li, M. X., and Sykes, B. D. (1998) Dynamics and thermodynamics of the regulatory domain of human cardiac troponin C in the apo- and calcium-saturated states, *Biochemistry 37*, 18032−18044.
40. Akke, M., Skelton, N. J., Kordel, J., Palmer, A. G., III, and Chazin, W. J. (1993) Effects of ion binding on the backbone dynamics of calbindin D9k determined by ^{15}N NMR relaxation, *Biochemistry 32*, 9832−9844.
41. Watterson, D. M., Sharief, F., and Vanaman, T. C. (1980) The complete amino acid sequence of the Ca^{2+}-dependent modulator protein (calmodulin) of bovine brain, *J. Biol. Chem. 255*, 962−975.
42. Shea, M. A., Verhoeven, A. S., and Pedigo, S. (1996) Calcium-induced interactions of calmodulin domains revealed by quantitative thrombin footprinting of Arg37 and Arg106, *Biochemistry 35*, 2943−2957.
43. Wimberly, B., Thulin, E., and Chazin, W. J. (1995) Characterization of the N-terminal half-saturated state of calbindin D_{9k}: NMR studies of the N56A mutant, *Protein Sci. 4*, 1045−1055.
44. Tada, M., Kobashigawa, Y., Mizuguchi, M., Miura, K., Kouno, T., Kumaki, Y., Demura, M., Nitta, K., and Kawano, K. (2002) Stabilization of protein by replacement of a fluctuating loop: Structural analysis of a chimera of bovine α-lactalbumin and equine lysozyme, *Biochemistry 41*, 13807−13813.
45. Permyakov, E. A., and Berliner, L. J. (2000) α-Lactalbumin: Structure and function, *FEBS Lett. 473*, 269−274.
46. Koch, A. W., Pokutta, S., Lustig, A., and Engel, J. (1997) Calcium binding and homoassociation of E-cadherin domains, *Biochemistry 36*, 7697−7705.
47. Shao, X., Fernandez, I., Sudhof, T. C., and Rizo, J. (1998) Solution structures of the Ca^{2+}-free and Ca^{2+}-bound C2A domain of synaptotagmin I: Does Ca^{2+} induce a conformational change? *Biochemistry 37*, 16106−16115.
48. Ubach, J., Zhang, X., Shao, X., Sudhof, T. C., and Rizo, J. (1998) Ca^{2+} binding to synaptotagmin: How many Ca^{2+} ions bind to the tip of a C2-domain? *EMBO J. 17*, 3921−3930.
49. Malmberg, N. J., Varma, S., Jakobsson, E., and Falke, J. J. (2004) Ca^{2+} activation of the cPLA2 C2 domain: Ordered binding of two Ca^{2+} ions with positive cooperativity, *Biochemistry 43*, 16320−16328.
50. Dudev, T., Chang, L. Y., and Lim, C. (2005) Factors governing the substitution of La^{3+} for Ca^{2+} and Mg^{2+} in metalloproteins: A DFT/CDM study, *J. Am. Chem. Soc. 127*, 4091−4103.
51. Drake, S. K., Zimmer, M. A., Miller, C. L., and Falke, J. J. (1997) Optimizing the metal binding parameters of an EF-hand-like calcium chelation loop: Coordinating side chains play a more important tuning role than chelation loop flexibility, *Biochemistry 36*, 9917−9926.
52. Renner, M., Danielson, M. A., and Falke, J. J. (1993) Kinetic control of Ca^{2+} signaling: Tuning the ion dissociation rates of EF-hand Ca^{2+} binding sites, *Proc. Natl. Acad. Sci. U.S.A. 90*, 6493−6497.

53. Drake, S. K., Lee, K. L., and Falke, J. J. (1996) Tuning the equilibrium ion affinity and selectivity of the EF-hand calcium binding motif: Substitutions at the gateway position, *Biochemistry 35*, 6697−6705.
54. Thompson, S. E., and Smithrud, D. B. (2002) Carboxylates stacked over aromatic rings promote salt bridge formation in water, *J. Am. Chem. Soc. 124*, 442−449.
55. Perl, D., and Schmid, F. X. (2001) Electrostatic stabilization of a thermophilic cold shock protein, *J. Mol. Biol. 313*, 343−357.
56. Wunderlich, M., Martin, A., and Schmid, F. X. (2005) Stabilization of the cold shock protein CspB from *Bacillus subtilis* by evolutionary optimization of Coulombic interactions, *J. Mol. Biol. 347*, 1063−1076.
57. Zhou, H. X., and Dong, F. (2003) Electrostatic contributions to the stability of a thermophilic cold shock protein, *Biophys. J. 84*, 2216−2222.
58. Henzl, M. T., and Graham, J. S. (1999) Conformational stabilities of the rat α- and *β*-parvalbumins, *FEBS Lett. 442*, 241−245.
59. Henzl, M. T., Larson, J. D., and Agah, S. (2000) Influence of monovalent cations on rat α- and *β*-parvalbumin stabilities, *Biochemistry 39*, 5859−5867.
60. Xiao, L., and Honig, B. (1999) Electrostatic contributions to the stability of hyperthermophilic proteins, *J. Mol. Biol. 289*, 1435−1444.

BI052508Q